JACS
JOURNAL OF THE AMERICAN CHEMICAL SOCIETY

COMMUNICATION

pubs.acs.org/JACS

Accurate Rates of the Complex Mechanisms for Growth and Dissolution of Minerals Using a Combination of Rare-Event Theories

Andrew G. Stack,*[,†] Paolo Raiteri,[‡] and Julian D. Gale[‡]

[†]Chemical Sciences Division, Oak Ridge National Laboratory, P.O. Box 2008, MS-6110, Oak Ridge, Tennessee 37831, United States
[‡]Nanochemistry Research Institute, Department of Chemistry, Curtin University, G.P.O. Box U1987, Perth, WA 6845, Australia

Supporting Information

ABSTRACT: Mineral growth and dissolution are often treated as occurring via a single reversible process that governs the rate of reaction. We show that multiple distinct intermediate states can occur during both growth and dissolution. Specifically, we used metadynamics, a method for efficiently exploring the free-energy landscape of a system, coupled to umbrella sampling and reactive flux calculations to examine the mechanism and rates of attachment and detachment of a barium ion onto a stepped barite ($BaSO_4$) surface. The activation energies calculated for the rate-limiting reactions, which are different for attachment and detachment, precisely match those measured experimentally during both growth and dissolution. These results can potentially explain anomalous non-steady-state mineral reaction rates observed experimentally and will enable the design of more efficient growth inhibitors and facilitate an understanding of the effect of impurities.

The ability to predict and control rates of reaction, impurity content, and morphologies of minerals and materials is applicable to diverse problems such as contaminant remediation, watershed and aquifer chemistry, new material design, and scale formation during oil, gas, and geothermal energy production. This has driven extensive research on the reaction mechanisms controlling the rates of growth and dissolution processes. While it is recognized that multiple bonds must break or form during growth and dissolution, these reactions have been treated in a practical sense as occurring via a single process with no intermediate species. That is, dissolved aqueous ions are treated as directly precipitating as the bulk mineral phase and vice versa dissolution, as in the following reaction written for barite:

$$BaSO_4(s) \rightleftarrows Ba^{2+}(aq) + SO_4^{2-}(aq) \quad (1)$$

Research on growth and dissolution has made substantial progress in identifying which surface structures on a solid are important, but a quantitative correlation between a specific rate-limiting chemical reaction and the net rate has been difficult to establish. Recent work has focused on atomistic computational techniques because of their ability to isolate specific reactions of interest. The challenges in using these techniques to obtain accurate rates and mechanisms are that the processes involved are often infrequent relative to the amount of time that can be practically simulated (rare events) and that it is necessary to account fully for the effect of the solvent and crystal structure on the interfacial reactions (many atoms). While coarse-grained approaches such as kinetic Monte Carlo can extend the range of length and time scales accessible to simulation, they still require accurate knowledge of the rate constants as input. These issues have led to computational estimates of crystal growth and dissolution reactions that differ from experiment by multiple orders of magnitude in just the activation energy alone, much less the rate.[1,2] Rare-event theories such as metadynamics[3] and reactive flux[4] have been used to model ion-pair formation,[5] water exchange,[6−8] and adsorption reactions,[9] making them potentially suitable for application to growth and dissolution. Free energies of attachment/detachment of ions to surfaces have sometimes been simulated as well.[10−14] In the present work, we have applied rare-event theories to mineral growth and dissolution and found that these processes do not necessarily consist of a single reaction but can include multiple intermediate species whose reactivity is not readily intuitable.

We examined barite both as a model compound to understand mineral reactions generally and because of the numerous instances where the ability to control and predict its growth and dissolution would be beneficial. For example, barite is the dominant scale-forming mineral in oil wells and reservoirs in the North Sea: the economic impact of scale formation on oil production worldwide has been estimated to be US $1.4 billion per year.[15] Barite is also able to incorporate metals such as radium into its crystal structure.[16] This is important due to the potential to immobilize contaminants through engineered growth of a mineral.[17] Lastly, barite dissolution rates display minimal pH dependence under circumneutral conditions, suggesting that dissociation of water plays a limited role.[18] This enables the application of classical Molecular Dynamics simulations with nondissociative potentials.

The addition or removal of the first ion to or from a monomolecular "step" (a dislocation in the continuity of a planar surface, as depicted in Figure 1) is a process known as "kink-site nucleation". This has been proposed to limit growth or dissolution near equilibrium on materials that sharply follow crystallographic orientations at the molecular level.[19] On barite, steps achieve maximum growth rates under solutions containing excess barium, suggesting that attachment of barium ions is rate-limiting in solutions containing stoichiometric amounts of barium and sulfate.[20] We therefore simulated the kink-site nucleation reaction for a barium ion adsorbed to a step aligned parallel to the [120] crystallographic direction, the dominant orientation found on barite {001} surfaces.

Technical details are listed in the Supporting Information (SI). Briefly, metadynamics is a technique that allows for fast exploration

Received: May 27, 2011
Published: July 01, 2011

dx.doi.org/10.1021/ja204714k | J. Am. Chem. Soc. 2012, 134, 11–14

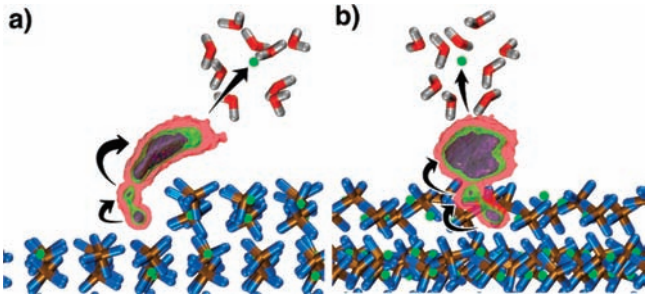

Figure 1. Metadynamics simulation of barium detachment from a monomolecular barite [120] step. Barium atoms are green, sulfate ions ochre (sulfur) and blue (oxygen), oxygens of water red, and hydrogens gray. (a) View along the [120] direction. The step-edge is in the middle, with terraces to the right and left. (b) View of the same image perpendicular to [120]. The colored areas are isosurfaces representing the free energies of various states relative to the starting configuration (the purple area closest to the lower terrace). The scale is 0−10 kJ/mol for purple, 10−17 kJ/mol for green, and 17−46 kJ/mol for red. The curved black arrows denote the reactions that are necessary prior to the breaking of all the bonds between the ion and the mineral surface.

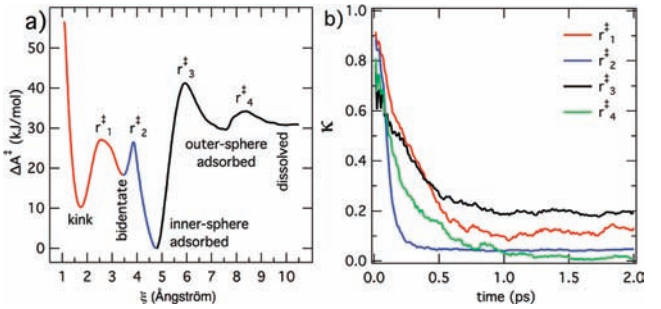

Figure 2. Results of umbrella sampling and reactive flux calculation. (a) Composite free-energy surface assembled from three separate free-energy surfaces (denoted by color; each is shown individually in Figure S1). The system includes four separate transition states (peaks $r^{\ddagger}_{1-4}$) between five energetically distinct species (valleys, each labeled with the name of the corresponding state). (b) Transmission coefficients for the four transition states. These describe the fraction of recrossings that occur at each transition state in (a).

of the free-energy landscape (surface). It is based on the choice of one or more reaction coordinates (called collective variables) and a penalty potential that forces the system to explore new regions of space.[3] Because of the low symmetry of the step edge, it was determined that three collective variables (the barium coordinates in x, y, and z) were necessary to determine the reaction mechanism unambiguously. Since achieving convergence could be extremely time-consuming, we used metadynamics to explore the reaction mechanism and a sequence of umbrella sampling calculations to obtain the free-energy surface.[21,22] This derived surface can be used to calculate a transition-state theory (TST) rate constant (k_{TST}). Next, we used the reactive flux method to perform stochastic sampling of the number of barrier recrossings from the transition state to calculate the transmission coefficient, κ.[4] The net rate constant for a reaction, k, is the product of k_{TST} and κ.

The results of the metadynamics simulations are shown in Figure 1 and presented as an animation in the SI (for the purpose of clarity, all water molecules except for those coordinating the dissolving barium ion have been omitted, although the surface was fully solvated). The starting configuration is the purple area closest to the lower terrace of the barite {001}. The higher-energy isosurfaces (green, then red) form saddle points between the lower-energy states (purple). Each saddle point indicates a transition state, and signify that the reaction is complex, passing through multiple energetically and structurally distinct intermediate states prior to dissolution. The composite free-energy surface derived from the umbrella sampling simulations is shown in Figure 2a (the individual sections are shown in Figure S1 in the SI). Each valley-to-peak energy difference is the free energy of activation ($\Delta A^{\ddagger}$) for a reaction. These vary substantially: some reactions have $\Delta A^{\ddagger}$ values of little more than thermal energy (2.5 kJ/mol at 300 K), whereas others have much larger values. Starting from the initial state, where the adsorbed barium forms five bonds to three sulfates on the step edge (Figure 3a), the system must pass through a +17 kJ/mol barrier. The bonds between the adsorbed barium and one of the sulfates on the lower terrace break, and the remaining two sulfates rotate in place to form the first intermediate, a bidentate arrangement (Figure 3b). From there, the system overcomes a small barrier

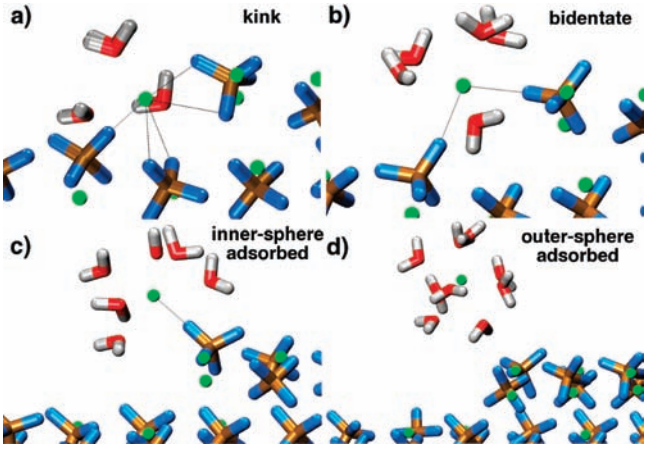

Figure 3. Structures of the stable states determined from the metadynamics and reactive flux calculations. Coloring of atoms is the same as in Figure 1. (a) Kink site, where the barium makes five bonds to three surface sulfates. (b) The first intermediate is a bidentate arrangement, where the departing barium makes two bonds, one to each of two surface sulfates. (c) An inner-sphere adsorbed species, involving only one bond to a surface sulfate, is then formed. This is the most stable species. (d) Immediately prior to completely dissolving, the last bond between the barium and the surface is broken, forming an outer-sphere adsorbed species.

($\Delta A^{\ddagger}$ = +8 kJ/mol) wherein the bond between the adsorbed barium ion and the remaining sulfate on the lower terrace is broken, forming a monodentate complex (Figure 3c). We will use the classical geochemical terminology and refer to this as an "inner-sphere" adsorbed species. The system then must climb a large barrier ($\Delta A^{\ddagger}$ = +41 kJ/mol) to break the final bond to the surface to form an fully solvated "outer-sphere" adsorbed species (Figure 3d). This is followed by facile ($\Delta A^{\ddagger}$ = +5 kJ/mol) detachment of the ion into the bulk solution, completing the dissolution. The attachment reaction can be taken as the reverse of the above (i.e., going from the surface to dissolved species to kink site). It has previously been shown that preadsorption of sulfate significantly enhances the rate of barium attachment to planar surfaces.[10] Here, it appears that the sulfate within the step edge that coordinates the attaching/detaching barium in the inner-sphere complex (Figure 3c) plays this role.

Table 1. Rate and Equilibrium Constants at 300 K[a]

reaction		k_{TST} (s^{-1})	k (s^{-1})	$\Delta A^{\ddagger}$ (kJ/mol)	κ	log K
kink ⇄ bidentate	det.	1.9×10^{9}	2.3×10^{8}	17	0.12	−2.0
	att.	2.0×10^{11}	2.4×10^{10}	9		
bidentate ⇄ IS_{ads}	det.	5.4×10^{10}	2.4×10^{9}	8	0.045	+3.4
	att.	**2.3×10^{7}**	**1.0×10^{6}**	**27**		
IS_{ads} ⇄ OS_{ads}	det.	**1.3×10^{5}**	**2.2×10^{4}**	**41**	0.17	−4.6
	att.	5.4×10^{9}	9.2×10^{8}	12		
OS_{ads} ⇄ dissolved	det.	5.4×10^{9}	9.2×10^{7}	5	0.017	−0.15
	att.	7.5×10^{9}	1.3×10^{8}	3		
overall						−3.4

[a] IS_{ads} and OS_{ads} are the inner-sphere adsorbed and outer-sphere adsorbed species. "att." and "det." stand for attachment and detachment, respectively. The rate-limiting reactions for detachment and attachment are highlighted in bold.

The rate-limiting reaction for detachment is the change of the ion from the inner-sphere to the outer-sphere adsorbed species, for which $\Delta A^{\ddagger}$ = +41 kJ/mol (Figure 2a). This result is surprising, since for mineral surface reactions one might assume *a priori* that breaking the first bond(s) to the surface would be rate-limiting because that is where the surface species is most constrained in its flexibility and where surface bonds are least available for attack by water. Our results demonstrate that for barite, breaking the *last* bond to the surface limits the rate. Additionally, the reverse is not true: formation of the first bond is not rate-limiting for attachment, nor is it the same reaction that limits the rate of detachment. The rate-limiting reaction for attachment is found to be the conversion of the inner-sphere adsorbed species to the bidentate species, for which $\Delta A^{\ddagger}$ = +27 kJ/mol. Since the rate-limiting reaction for both attachment and detachment involves escape of the ion from the inner-sphere adsorbed species, the model favors this species over all others. Although this state has the lowest energy in Figure 2a, it should be remembered that this is relative to those sampled, with the bulk and flat surface being lower again. It is these more stable states that ultimately drive the net growth or dissolution of the system.

The values of κ, k_{TST}, and k for each reaction are shown in Table 1. For the transmission coefficient (Figure 2b), there is a rough correlation between its magnitude and $\Delta A^{\ddagger}$: the smaller $\Delta A^{\ddagger}$ is in either the forward or reverse direction, the smaller the value of κ. This can be understood by recognizing that κ represents the degree of barrier recrossing.[4] In general, a small energetic barrier in the forward or reverse direction leads to a large number of recrossings and thus a reduction in the transmission coefficient. However, the overall rate constant is still large for these reactions, since k_{TST} is large. The range of the rate constants at 300 K spans nearly 6 orders of magnitude, with a ceiling for reactions that are diffusion limited ($k = 10^{9}$–10^{10} s^{-1}). This complex reactivity can be analyzed through numerical simulation to probe its relaxation time, that is, the time required for the concentration of the product to reach $1/e$ times its equilibrium value. The relaxation time of the system simulated here was 0.5 μs, assuming a batch reactor equilibrating with a fixed concentration of barite (data shown in Figure S2). The rate of dissolution during this equilibration does not asymptotically decay to zero but instead rapidly increases to a maximum, which is followed by a slow decay. This pattern of reactivity has been observed experimentally for barite nanoparticles in aqueous solutions, but on a time scale of hours.[23]

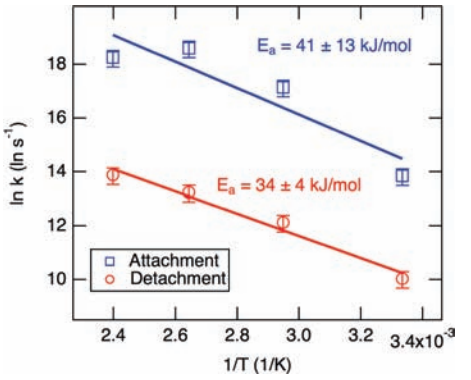

Figure 4. Arrhenius plots for the rate-limiting reactions for detachment and attachment. The activation energies for attachment and detachment match the experimental estimates of the activation energies for step growth and dissolution, respectively. Error bars are ±30% of the rate constant, as derived from ref 26.

We simulated the temperature dependence of the rate-limiting reactions for detachment and attachment and created an Arrhenius plot for k (i.e., ln k vs $1/T$) (Figure 4; individual calculations at the various temperatures are shown in Figure S1). We calculated only the temperature dependence of the rate-limiting reactions because of practical restraints on simulation time, but these ought to reflect the activation energies measured under steady-state conditions. The Arrhenius activation energy for the rate-limiting detachment reaction is 34 ± 4 kJ/mol, which is identical to the experimentally measured activation energy for dissolution of the [120] step edge observed microscopically.[24] The exact agreement between the experimental and computational estimates strongly suggests that this study has accurately captured the rate-limiting reaction for dissolution. Furthermore, this remarkable consistency supports the assertion that multiple reactions occur during mineral growth and dissolution. Since the rate-limiting reaction for detachment is the breaking of the last bond to the surface, the starting structure used here does not necessarily need to be correct. That is, during dissolution of a material whose steps strongly follow crystallographic directions, one would expect that detachment of the first ion from an otherwise smooth step would limit the dissolution rate.[19] Nucleation of a negative kink site would then be rate-limiting, as opposed to the detachment from a positive kink site simulated here. However, it could be the case that detachment of an inner-sphere adsorbed species is rate-limiting regardless of what surface structure on the step initiates the dissolution process.

For growth, the experimentally determined activation energy for [120] step advance is 38 ± 5 kJ/mol.[25] Our estimate of the Arrhenius activation energy for the rate-limiting attachment reaction is 41 ± 13 kJ/mol (Figure 4), again in quantitative agreement with the experimental result. However, the non-Arrhenius nature of the calculated activation energy for attachment, produces a large uncertainty in the estimate. It is likely that there is a shift in the interfacial water structure with temperature that disproportionately affects this reaction. That is, this model predicts that an intricate water structure interacts with the {001} barite surface (which includes the [120] steps), where oxygens and hydrogens of water coordinate barium and sulfate ions, respectively.[26] The coordination numbers of barium and sulfate ions are likely to change with temperature, and this could lead to a reorganization of the interfacial water, thus creating the non-Arrhenius nature of this reaction.

dx.doi.org/10.1021/ja204714k | *J. Am. Chem. Soc.* 2012, 134, 11–14

The ratio of the integrals of the free-energy surfaces for the attachment and detachment reactions can be used to calculate equilibrium constants,[27] K (Table 1). The overall equilibrium constant is the product of the constants for individual reactions:

$$K_{\text{overall}} = K_1K_2K_3K_4 = \frac{[\text{Ba}^{2+}]}{[\text{kink}]} \quad (2)$$

K_{overall} is $10^{-3.4}$ at 300 K. A value less than unity indicates that the kink site is energetically favored over the dissolved species. If differences between activity and concentration are ignored and the kink site is set as the standard state with a concentration equal to 1, the system predicts an aqueous barium concentration of $[\text{Ba}^{2+}] = 10^{-3.4}$ mol/L. Although detachment energies are not known experimentally, the estimate can be compared to the solubility product of barite,

$$K_{\text{sp}} = \frac{a_{\text{Ba}^{2+}(\text{aq})}a_{\text{SO}_4{}^{2-}(\text{aq})}}{a_{\text{BaSO}_4(\text{s})}} \approx [\text{Ba}^{2+}]^2 \quad (3)$$

Since the activity of barite, $a_{\text{BaSO}_4(\text{s})}$, can be set to 1, the solubility product is approximately equal to the square of the equilibrium concentration of aqueous barium ion. The experimental estimate of the K_{sp} value is $10^{-9.94}$ at 300 K,[28] which yields $[\text{Ba}^{2+}] \approx 10^{-4.97}$ mol/L. It is likely that the discrepancy between the calculated and experimental estimates is due to the fact that only a single surface site was simulated here out of many: the experimentally measured net solubility product may reflect other surface structures or the contribution of sulfate ions.

Beyond the simulation of accurate rates of growth and dissolution, this work has significant implications for mineral growth and dissolution generally: the observation of multiple intermediate states may potentially explain anomalous, non-steady-state reaction rates. Examples of this effect include dissolution rates that increase to a maximum and then decay to a steady-state rate[23,29] and dissolution rates that decay over time and only slowly approach a steady state.[30−32] If the amount of material found to react anomalously corresponds to less than a monolayer of material,[29] this would suggest that morphology or reactive surface area changes cannot be the driving force for the anomalous reactivity. Our results suggest that if an adsorbed species is labile or recalcitrant relative to the bulk, it will react at a different rate than the mineral surface itself and produce anomalous dissolution and/or growth behavior. The time scale of this effect will depend on the character of the material, with covalently bonded materials expected to react more slowly. Lastly, the design of growth inhibitors[33] should consider the rate-limiting reaction in dissolution. It is clear that a growth inhibitor that acts by further stabilizing the inner-sphere adsorbed complex or preventing its formation will have a strong inhibitory effect on the rate of growth of barite.

■ ASSOCIATED CONTENT

Supporting Information. Detailed accounts of the methodology, equations, simulation parameters, and potentials of mean force and an animated version of Figure 1 (QT). This material is available free of charge via the Internet at http://pubs.acs.org.

■ AUTHOR INFORMATION

Corresponding Author
stackag@ornl.gov

■ ACKNOWLEDGMENT

This research was sponsored by the Division of Chemical Sciences, Geosciences, and Biosciences, Office of Basic Energy Sciences, U.S. Department of Energy (A.G.S.) and the Australian Research Council through Discovery Grant DP0986999 (P.R. and J.D.G.). The authors thank David J. Wesolowski, Paul R. C. Kent, and two anonymous reviewers for helpful comments.

■ REFERENCES

(1) Elhadj, S.; Salter, E. A.; Wierzbicki, A.; De Yoreo, J. J.; Han, N.; Dove, P. M. *Cryst. Growth Des.* **2006**, *6*, 197.
(2) Stack, A. G. *J. Phys. Chem. C* **2009**, *113*, 2104.
(3) Laio, A.; Parrinello, M. *Proc. Natl. Acad. Sci. U.S.A.* **2002**, *99*, 12562.
(4) Chandler, D. In *Classical and Quantum Dynamics in Condensed Phase Simulations*; Berne, B. J., Ciccotti, G., Coker, D. F., Eds.; World Scientific: Singapore, 1997.
(5) Rey, R.; Guàrdia, E. *J. Phys. Chem.* **1992**, *96*, 4712.
(6) Spångberg, D.; Rey, R.; Hynes, J. T.; Hermansson, K. *J. Phys. Chem. B* **2003**, *107*, 4470.
(7) Wang, J.; Rustad, J. R.; Casey, W. H. *Inorg. Chem.* **2007**, *46*, 29620.
(8) Kerisit, S.; Rosso, K. M. *J. Chem. Phys.* **2009**, *131*, No. 114512.
(9) Kerisit, S.; Parker, S. C. *J. Am. Chem. Soc.* **2004**, *126*, 10152.
(10) Piana, S.; Jones, F.; Gale, J. D. *J. Am. Chem. Soc.* **2006**, *128*, 13568.
(11) Spagnoli, D.; Kerisit, S.; Parker, S. C. *J. Cryst. Growth* **2006**, *294*, 103.
(12) Raiteri, P.; Gale, J. D.; Quigley, D.; Rodger, P. M. *J. Phys. Chem. C* **2010**, *114*, 5997.
(13) Pina, C. M.; Becker, U.; Risthaus, P.; Bosbach, D.; Putnis, A. *Nature* **1998**, *395*, 483.
(14) Becker, U.; Risthaus, P.; Bosbach, D.; Putnis, A. *Mol. Simul.* **2002**, *28*, 607.
(15) Frenier, W. W.; Ziauddin, M. *Formation, Removal, and Inhibition of Inorganic Scale in the Oilfield Environment*; Society for Petroleum Engineers: Richardson, TX, 2008.
(16) Curti, E.; Fujiwara, K.; Iijima, K.; Tits, J.; Cuesta, C.; Kitamura, A.; Glaus, M. A.; Müller, W. *Geochim. Cosmochim. Acta* **2010**, *74*, 3553.
(17) Tartakovsky, A. M.; Redden, G.; Lichtner, P. C.; Scheibe, T. D.; Meakin, P. *Water Resour. Res.* **2008**, *44*, No. W06S04.
(18) Dove, P. M.; Czank, C. A. *Geochim. Cosmochim. Acta* **1995**, *59*, 1907.
(19) De Yoreo, J. J.; Zepeda-Ruiz, L .A.; Friddle, R. W.; Qiu, S. R.; Wasylenki, L. E.; Chernov, A. A.; Gilmer, G. H.; Dove, P. M. *Cryst. Growth Des.* **2009**, *9*, 5135.
(20) Kowacz, M.; Putnis, C. V.; Putnis, A. *Geochim. Cosmochim. Acta* **2007**, *71*, 5168.
(21) Torrie, G. M.; Valleau, J. P. *J. Comput. Phys.* **1977**, *23*, 187.
(22) Ensing, B.; Klein, M. L. *Proc. Natl. Acad. Sci. U.S.A.* **2005**, *102*, 6755.
(23) Vogelsberger, W.; Schmidt, J. *J. Phys. Chem. C* **2011**, *115*, 1388.
(24) Higgins, S. R.; Jordan, G.; Eggleston, G.; Knauss, K. G. *Langmuir* **1998**, *14*, 4967.
(25) Higgins, S. R.; Bosbach, D.; Eggleston, C. M.; Knauss, K. G. *J. Phys. Chem. B* **2000**, *104*, 6978.
(26) Stack, A. G.; Rustad, J. R. *J. Phys. Chem. C* **2007**, *111*, 16387.
(27) Chialvo, A. A.; Cummings, P. T.; Cochran, H. D.; Simonson, J. M.; Mesmer, M. E. *J. Chem. Phys.* **1995**, *103*, 9379.
(28) Felmy, A. R.; Rai, D.; Amonette, J. E. *J. Solution Chem.* **1990**, *19*, 175.
(29) Samson, S. D.; Stillings, L. L.; Eggleston, C. M. *Geochim. Cosmochim. Acta* **2000**, *64*, 3471.
(30) Bandstra, J. Z.; Brantley, S. L. *Geochim. Cosmochim. Acta* **2008**, *72*, 2587.
(31) Knauss, K. G.; Wolery, T. J. *Geochim. Cosmochim. Acta* **1988**, *52*, 43.
(32) Jordan, G.; Pokrovsky, O. S.; Bahlo, J.; Guichet, X.; Schlueter, C. *Chem. Geol.* **2011**, *286*, 272.
(33) Bosbach, D.; Coveney, P. V.; Griffin, J. L. W.; Putnis, A.; Risthaus, P.; Stackhouse, S.; Whiting, A. *J. Chem. Soc., Perkin Trans. 2* **2002**, 1238.